PASSIVE LC SENSORS - AN ANALYSIS

A Project Report

submitted by

TEJA VYAS GUTTAVALLI

EE16B122

in partial fulfilment of the requirements

for the award of the degree of

BACHELOR OF TECHNOLOGY

&

MASTER OF TECHNOLOGY

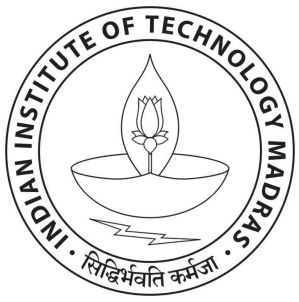

DEPARTMENT OF ELECTRICAL ENGINEERING

INDIAN INSTITUTE OF TECHNOLOGY MADRAS.

JUNE 2021

THESIS CERTIFICATE

This is to certify that the thesis titled **PASSIVE LC SENSORS - AN ANALYSIS**, submitted by **Teja Vyas Guttavalli**, to the Indian Institute of Technology, Madras, for the award of the degree of **Bachelor of Technology & Master of Technology**, is a bonafide record of the project work done by him under our supervision. The contents of this thesis, in full or in parts, have not been submitted to any other Institute or University for the award of any degree or diploma.

Prof.Boby George
Project Guide
Professor
Dept. of Electrical Engineering
IIT-Madras, 600 036

Place: Chennai

Date: June 2021

ACKNOWLEDGEMENTS

First and foremost, I would like to express my profound gratitude and thankfulness to my project guide, **Dr. Boby George**, Department of Electrical Engineering, IIT Madras for his invaluable guidance and support throughout the entire course of my project. I am highly indebted to him for devoting his valuable time and for his unreserved cooperation. Working under him was a pleasant learning experience and I sincerely thank him for giving me this opportunity.

I would like to thank my family and friends at IITM who unconditionally supported and encouraged me at every step of this wonderful journey. Above all, I thank God for his grace that made me the person I am today.

ABSTRACT

KEYWORDS: Passive LC sensor, coupling, mutual inductance, Readout schemes, interference, frequency response

Wireless passive sensors are one of the key modules in a number of non-contact measurement applications. One of the simple types of wireless passive sensor is an inductive coupling based LC resonator.

Our work focuses on the effects of noise on this system and how can they be quantified. Also as the coupling coefficient plays a major role, our work shall also focus on maximum operable distance between inductive coils.

TABLE OF CONTENTS

ACKNOWLEDGEMENTS **i**

ABSTRACT **ii**

LIST OF FIGURES **iv**

NOTATION **v**

1 INTRODUCTION **1**

1.1 Passive LC sensor 1

1.2 Objective 2

1.3 Thesis Organization 2

2 WIRELESS LC SENSING - AN ANALYSIS **3**

2.1 Readout schemes based on Frequency Response 3

2.2 Change in Magnitude response 5

2.3 Change in phase response 7

2.4 Effect of coupling coefficient 7

2.5 Maximum operable distance for two planar square coils 10

2.5.1 Self Inductance 11

2.5.2 Mutual Inductance 12

2.5.3 Coupling coefficient vs distance 13

2.5.4 Code written for calculation of k 14

2.6 Readout scheme based on FFT 16

3 CONCLUSION **19**

A REFERENCES **20**

LIST OF FIGURES

1.1 A typical Passive LC sensor 1

2.1 Circuit of a passive LC sensor 3
2.2 Equivalent circuit 4
2.3 Magnitude response of I_1 5
2.4 Phase response of I_1 5
2.5 Change in f_p with C_x 6
2.6 Change in phase response with respect to C_x 8
2.7 Change of phase response with respect to k 9
2.8 Planar square coil 11
2.9 Coupling coefficient Vs Distance 13
2.10 Circuit of the readout scheme based on FFT 16
2.11 Output voltage obtained across the resistor R_s 17
2.12 Maximum occurs at parallel resonance frequency 18
2.13 Peaks around f_p when noise is added and the Fitted curve in red[3] 18

NOTATION

ρ	Radius of a wire
L	Self Inductance of a coil
M	Mutual Inductance between coils
C	Capacitance
k	Coupling Coefficient
f_s	Series Resonance Frequency
f_p	Parallel Resonance Frequency
ϕ	Phase
δ_{xy}	Gap between two wires
D_{xy}	Distance between centres of two wires
a	Length of coil
N	Number of turns
FFT	Fast Fourier Transform

CHAPTER 1

INTRODUCTION

The presence of sensors has become quite ubiquitous these days. Wireless sensors play a prominent role in our day to day life with the emergence of technologies like Internet of things(IoT).

Wireless Passive LC sensors are one of the simple types of wireless sensors that are used in several applications like pH monitoring, monitoring of concrete structures, measurement of humidity, monitoring wound health through bandages, sensing intra-ocular pressure, patient health monitoring and strain monitoring of automobile tyre.

1.1 Passive LC sensor

A wireless passive LC sensor system consists of two magnetically coupled coils. One of the coils, referred as sensor coil, is connected to a capacitive sensor and forms an LC tank circuit. The second coil, called as readout coil is electrically connected to measurement circuit. The resonance frequency of the circuit changes with the capacitive sensor C_x . Such systems are particularly useful when physical access to the sensing element is limited.

Fig. 1.1 shows the circuit of a typical passive LC sensor. L_1 is the self inductance of readout coil, L_2 is the self inductance of sensor coil. C_x is the capacitive sensor. The

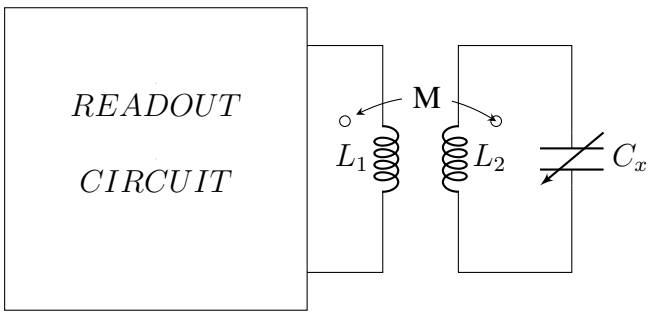

Figure 1.1: A typical Passive LC sensor

sensor coil and the read out coil are magnetically coupled. Their mutual inductance is M, where

$$M = k\sqrt{L_1 \times L_2} \tag{1.1}$$

The readout circuit is where the unknown capacitance C_x is measured. It depends on the readout scheme that's used.

1.2 Objective

There are different readout techniques for passive LC sensors and noise has different effects depending on the technique used. Our work involves analysing those effects due to noise and quantifying them.

1.3 Thesis Organization

We shall study different readout techniques and the effects of noise on them. Apart from noise, mutual inductance also affects readout schemes. Therefore we shall analyze those effects and implement a code that calculates mutual inductance of two square coils.

CHAPTER 2

WIRELESS LC SENSING - AN ANALYSIS

The sensing element in our circuit is the capacitor C_x, refer Fig. 2.1. The frequency response of the circuit changes with the change in C_x. There are many readout schemes depending on the changes in frequency response. Different readout schemes use different attributes of the circuit.

2.1 Readout schemes based on Frequency Response

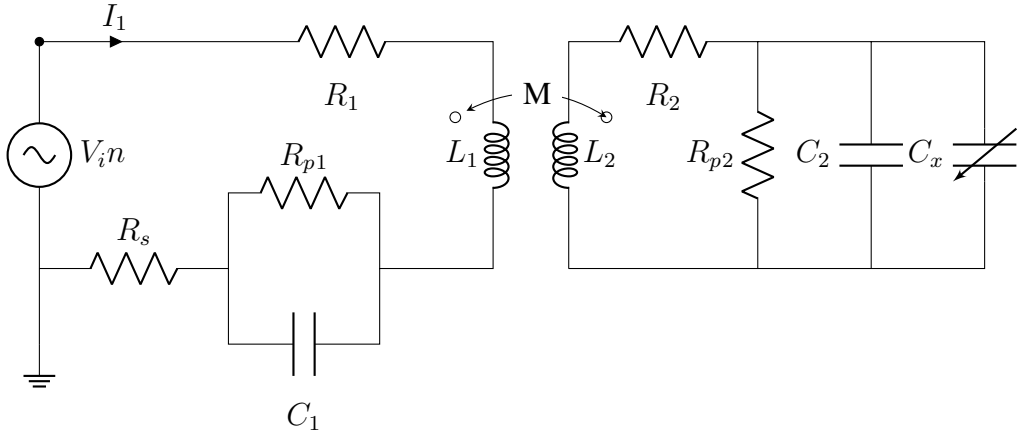

Figure 2.1: Circuit of a passive LC sensor

In fig. 2.1, L_1 is the self inductance of readout coil, R_1 is its resistance. A capacitor C_1 is connected in series to L_1 and R_{p1} is its leakage capacitance. L_2 is the self inductance of sensor coil, R_2 is its resistance. The sensor coil and the read out coil are magnetically coupled. Their mutual inductance is M. A fixed known capacitor C_2 is connected parallel to C_x across L_2. C_x is the capacitive sensor and with the change in C_x the resonance frequency of the circuit changes.

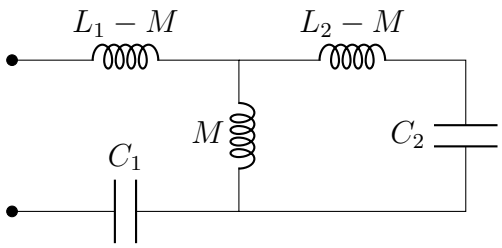

Figure 2.2: Equivalent circuit

Fig. 2.2 is the electrical equivalent of the circuit mentioned in Fig. 2.1. It is the equivalent T-model of the system with $C_X = 0$ and neglecting coil resistances and leakage resistances. The equivalent impedance $Z(j\omega)$ across the terminals can be written as

$$Z(j\omega) = \frac{L_1C_1L_2C_2(1-k^2)\omega^4 - (L_1C_1 + L_2C_2)\omega^2 + 1}{j\omega C_1(1 - L_2C_2\omega^2)} \tag{2.1}$$

The numerator can be expressed as product of $(\omega_{s1}^2 - \omega^2)$ and $(\omega_{s2}^2 - \omega^2)$. Therefore the system has two series resonance frequencies and one parallel resonance frequency. If we assume $L_1C_1 = L_2C_2$ Then

$$f_{s1}, f_{s2} = \frac{1}{2\pi}[L_2C_2(1 \pm k)]^{-1/2} \tag{2.2}$$

where f_{s1} and f_{s2} are series resonance frequencies and k is the coupling coefficient[1]. The difference between them reduces if the value of k reduces.
The parallel resonance frequency can be written as

$$f_p = \frac{1}{2\pi}[L_2C_2]^{-1/2} \tag{2.3}$$

I_1 is the current flowing through the readout coil. For an input voltage V_in, I_1 can be written as

$$I_1(j\omega) = V_in(j\omega)/Z(j\omega)$$

The magnitude and phase plots of I_1 are shown in Fig. 2.3 and Fig. 2.4 respectively.

L_1	R_1	C_1	L_2	R_2	C_2	R_p
$56\mu H$	0.6Ω	$414pF$	$23.2\mu H$	0.4Ω	$996pF$	$460k\Omega$

Table 2.1: Circuit parameters

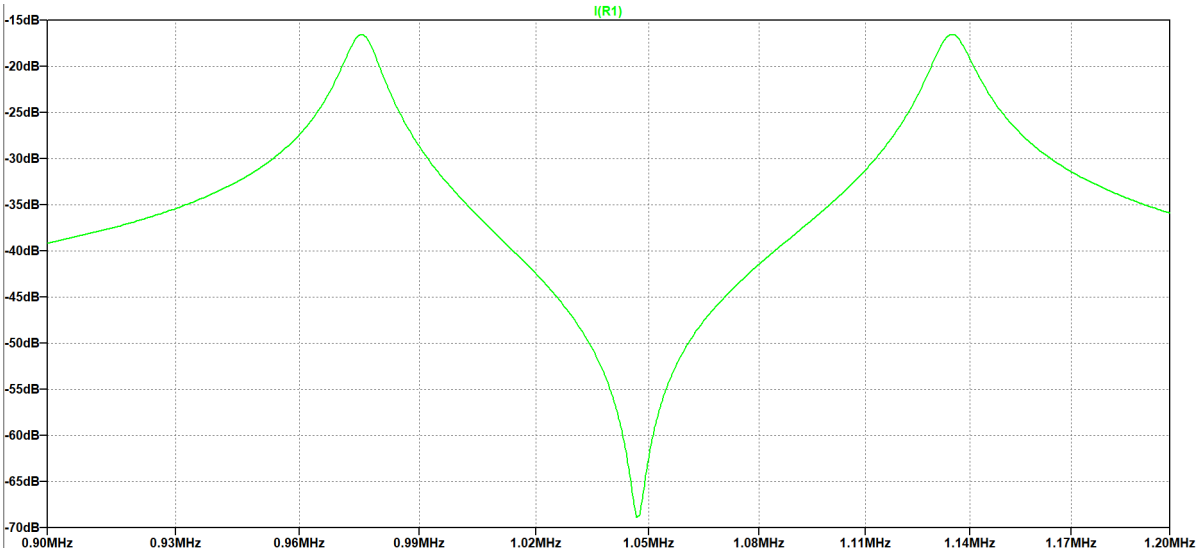

Figure 2.3: Magnitude response of I_1

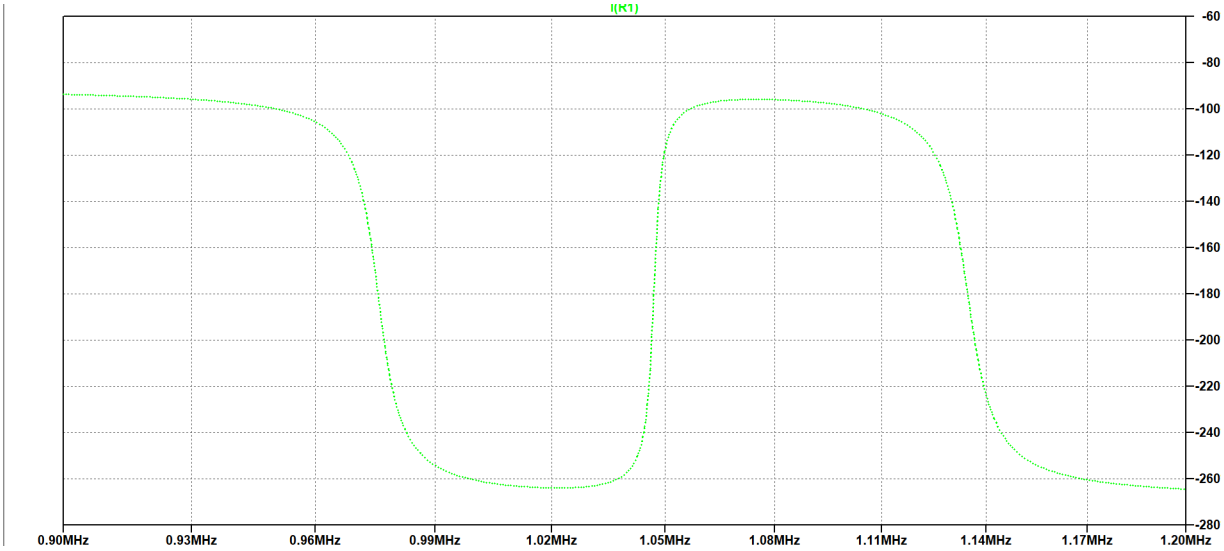

Figure 2.4: Phase response of I_1

These plots are obtained for $k = 0.15$ with the circuit parameters mentioned in table 2.1.The plots presented are obtained using SPICE tool LTspice XVII.
For a given k, as the value of C_x changes, the parallel resonance requency changes since it is dependent on C_2, the phase plot is also affected. We exploit these in our readout schemes.

2.2 Change in Magnitude response

C_x is connected across C_2 Therefore with change in C_x, f_p changes. There

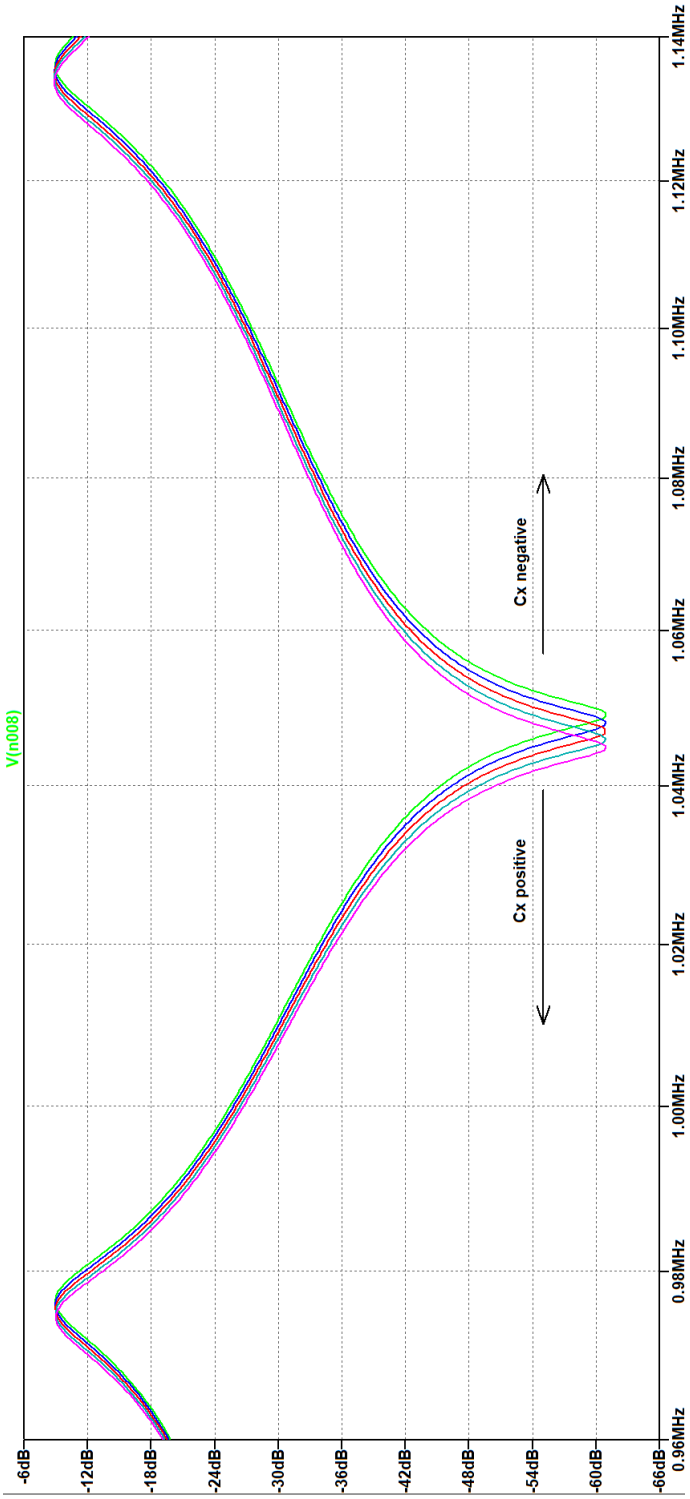

Figure 2.5: Change in f_p with C_x

are different readout schemes that detect the shift in resonance frequency and use appropriate readout electronics to calculate C_x. Fig. 2.5 is obtained by changing C_x from $-4pF$ to $4pF$ in the steps of $2pF$. As the value of f_p majorly depends on the values of L_2, C_2 and other circuit components. The effect of interference of external noise at the source does not affect the readout scheme. But the time taken for measurement is the concern. For every calculation we need to perform a frequency sweep, therefore it does not allow fast update rates. And also readout circuitry needed to detect the frequency shift is also complex. Though these readout circuits provide high signal to noise ratios, if C_x changes fast, they cannot be preferred.

2.3 Change in phase response

As seen in case of magnitude response, the phase response also changes with C_x. Fig. 2.1 is a readout scheme that uses phase change to sense the change in C_x. In this method, we do all the measurements at f_p. So it reduces the measurement time. We calculate the change in the tangent of phase. If we calculate the tangent of the measured phase, we get

$$\tan\phi = -\frac{[1-(\frac{\omega}{\omega_p})^2]}{\frac{2\zeta\omega}{\omega_p}} \tag{2.4}$$

$$\frac{d(\tan\phi)}{d\omega}|_{\omega=\omega_p+\Delta\omega} = \frac{-\Delta\omega/\omega_p}{\zeta\omega_p} + \frac{1}{\zeta\omega_p} \tag{2.5}$$

$\tan\phi$ has a linear relation with $\Delta\omega$ and $\Delta\omega$ varies linearly with ΔC_x[1]. Therefore we can measure C_x. The interference of external noise does not have effect on this readout scheme because it also depends mostly on the circuit elements. But there is another factor that plays a major role. Until now we did not consider the coupling coefficient. The value of coupling coefficient is important in phase related readout schemes. We shall discuss more about it in the next section.

2.4 Effect of coupling coefficient

The readout schemes are also affected by the coupling coefficient apart from noise. If the value of k reduces, the difference between f_{s1} and f_{s2} decreases and the

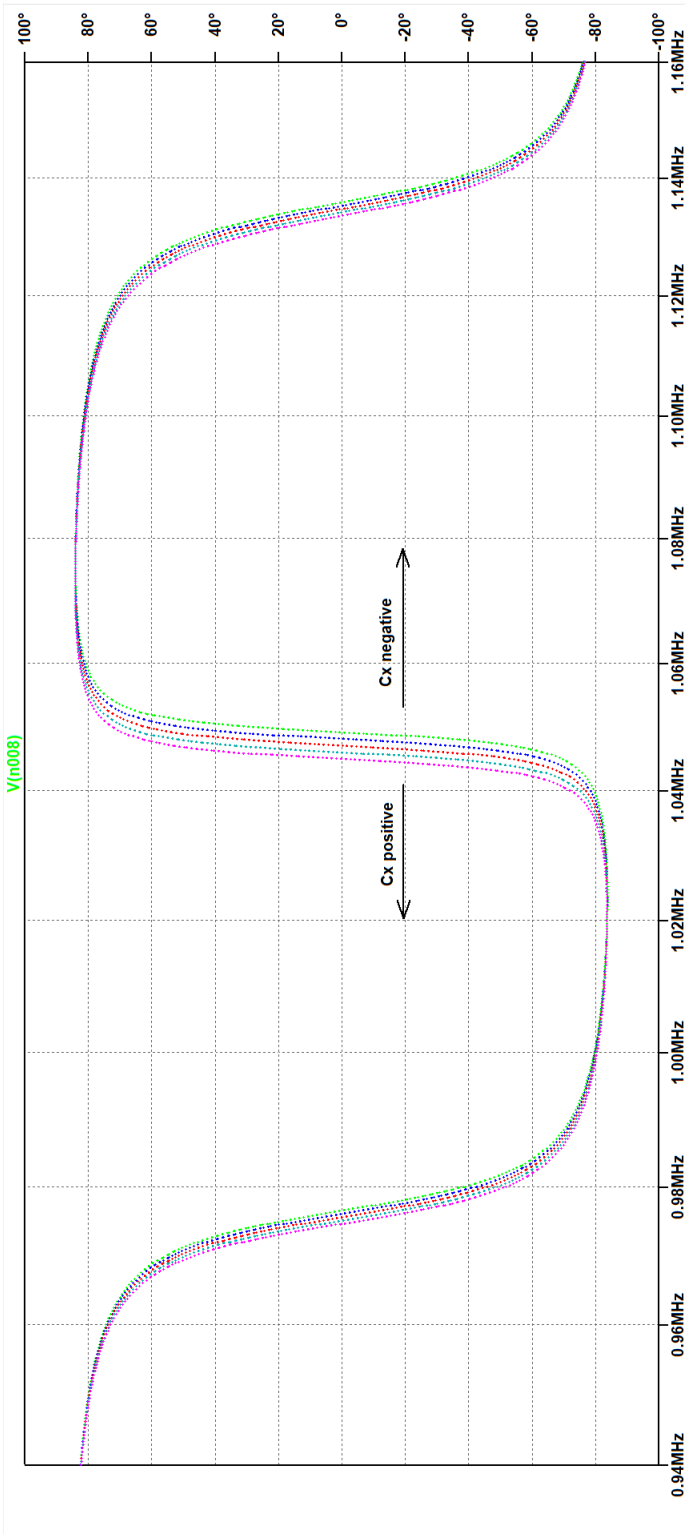

Figure 2.6: Change in phase response with respect to C_x

phase change at f_p gets affected. This results in inaccuracy if phase related readout schemes are implemented.

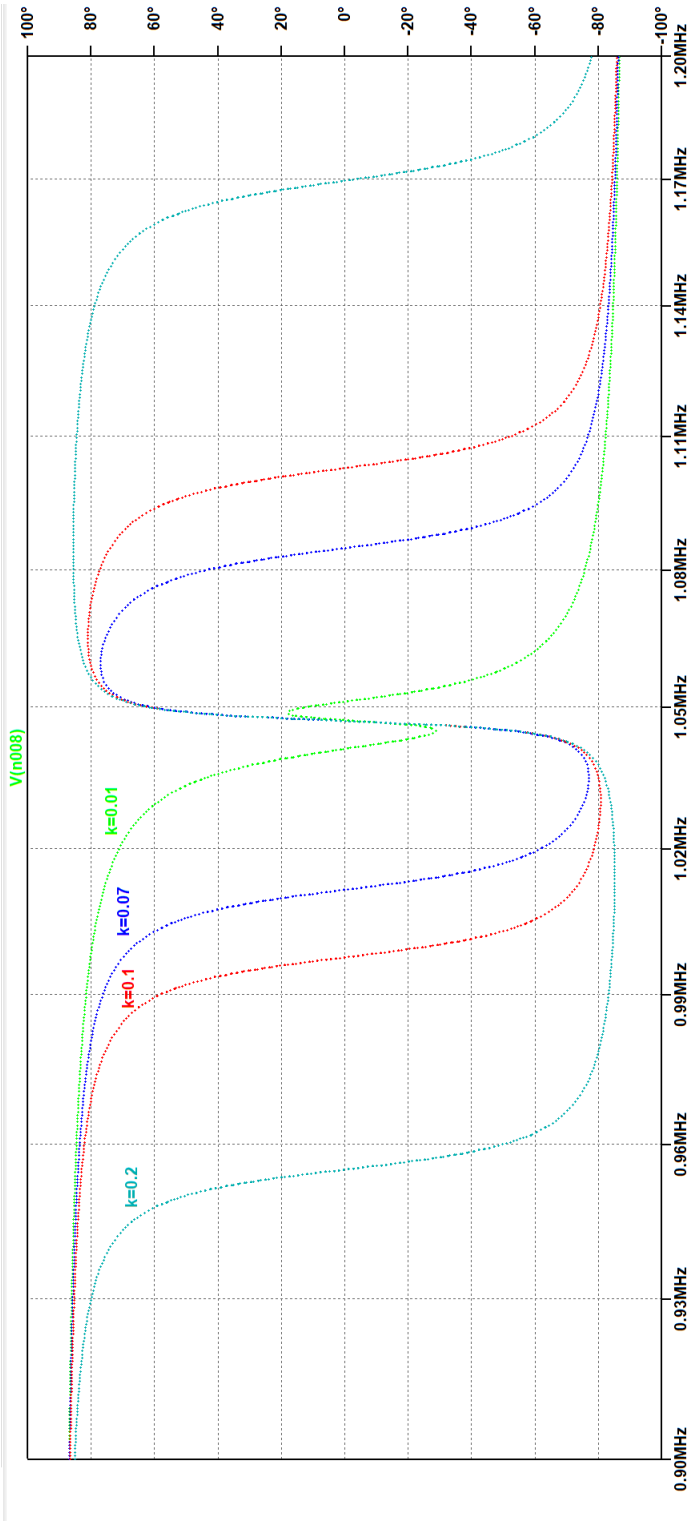

Figure 2.7: Change of phase response with respect to k

Fig. 2.7 shows the phase response of the circuit for k = 0.01, 0.07, 0.1, 0.2. For the circuit parameters used, it is found that for $k \geq 0.1$ everything around f_p

remained same whereas for $k < 0.1$ the slope changed due to the phase contributions of f_{s1} and f_{s2}. Therefore we need to make sure that k is above 0.1.
From eq. 1.1 we can write

$$k = \frac{M}{\sqrt{L_1 L_2}}$$

L_1 and L_2 are self inductances. They are only dependent on physical properties of the coils. Whereas M, mutual inductance, depends on the distance between the coils. As the distance between coils increases, mutual inductance decreases, resulting in the decrease of the value of k. Therefore there is a maximum operable distance so that the system can operate at minimum operable k or above.

2.5 Maximum operable distance for two planar square coils

In this section, we'll calculate the maximum operable distance for two planar square coils. For that we need to calculate the self inductance of the coil and mutual inductance between the coils.
For this calculation we need two initial equations. The self inductance of a straight conductor and mutual inductance between two equal and parallel straight conductors lying in the same plane.
The self inductance L of straight round copper wire of length l and radius ρ is given by[4].

$$L(l,\rho) = \frac{\mu_0}{4\pi} 2[l.\ln\frac{(l+\sqrt{l^2+\rho^2})}{\rho} - \sqrt{l^2+\rho^2} + \frac{l}{4} + \rho] \tag{2.6}$$

The mutual inductance between two straight conductors each of length l with a distance d between them and aligned perfectly is given by

$$M(l,d) = \frac{\mu_0}{4\pi} 2[l.\ln(\frac{l+\sqrt{l^2+d^2}}{d}) - \sqrt{l^2+d^2} + d] \tag{2.7}$$

Let us assume that the length of the side of each square coil is a. Radius of each wire is ρ, distance between two adjacent wires in a coil is δ_{xy}. Let the number of turns be N.D_{xy} be the distance between the centres of two adjacent wires. Therefore
D_{xy} = 2ρ + δ_{xy}.

2.5.1 Self Inductance

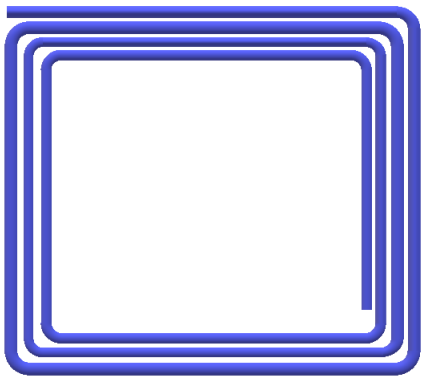

Figure 2.8: Planar square coil

The coil we used is a square. If the self inductance of each side is L_{side}, then self inductance of the coil, L_{coil}, will be four times L_{side}. L_{side} can be written as

$$L_{side} = L_{\omega} + M_{ss} - M_{os} \tag{2.8}$$

L_{ω} is the sum of self inductances of each wire present on one side of coil.

$$L_{\omega} = \sum_{i=0}^{N-1} L(l_i, \rho) \tag{2.9}$$

l_0 will be outermost turn with length a. The length of adjacent turn will be less by $2D_{xy}$. Therefore

$$l_i = a - 2iD_{xy} \tag{2.10}$$

In eq. 2.8, M_{ss} is the sum of mutual inductances between wires present on the same side of the coil.

$$M_{ss} = \sum_{i=0}^{N-1} \sum_{i=0; i' \neq i}^{N-1} M(\bar{a}, d_{i-i'}) \tag{2.11}$$

where $\bar{a}$ is the averaged length of wires in the side and $d_i - i'$ is the appropriate distance between the wires. $\bar{a} = a_0 - (N-1)D_{xy}$.

In eq. 2.8, M_{os} is the sum of mutual inductances between the wires present in the opposite sides of the same coil. We do not add the effect of adjacent wires because the current in them travels perpendicularly resulting in no effect and the negative sign before M_{os} comes because of the fact that current travels in opposite directions in the

opposite sides of the coil. Therefore

$$M_{os} = \sum_{i=0}^{N-1} \sum_{j=0}^{N-1} M(\bar{a}, d_{ij}) \tag{2.12}$$

where d_{ij} is the appropriate distance between the wires.

Combining all the above equations we have[4]

$$L_{coil} = 4(\sum_{i=0}^{N-1} L(l_i, \rho) + \sum_{i=0}^{N-1} \sum_{i=0;i' \neq i}^{N-1} M(\bar{a}, d_{i-i'}) + \sum_{i=0}^{N-1} \sum_{j=0}^{N-1} M(\bar{a}, d_{ij})) \tag{2.13}$$

2.5.2 Mutual Inductance

Mutual inductance, M, can be calculated in the same way as Self inductance. We first calculate M_{side}. It has two components M_1 and M_2

$$M_{side} = M_1 - M_2 \tag{2.14}$$

M_1 is the mutual inductance between the wires that are on the same side of both the coils.

$$M_1 = \sum_{i=0}^{N-1} \sum_{k=0}^{N-1} M(\bar{a}, d_{ik}) \tag{2.15}$$

where d_{ik} is the appropriate distance between the wires.

M_2 is the mutual inductance between the wires that are present on one side of the coil and opposite side on the other coil.

$$M_2 = \sum_{i=0}^{N-1} \sum_{t=0}^{N-1} M(\bar{a}, d_{it}) \tag{2.16}$$

where d_{it} is the appropriate distance between the wires. Therefore Mutual inductance between the coils will be[4]

$$M_{coil} = 4(\sum_{i=0}^{N-1} \sum_{k=0}^{N-1} M(\bar{a}, d_{ik}) - \sum_{i=0}^{N-1} \sum_{t=0}^{N-1} M(\bar{a}, d_{it})) \tag{2.17}$$

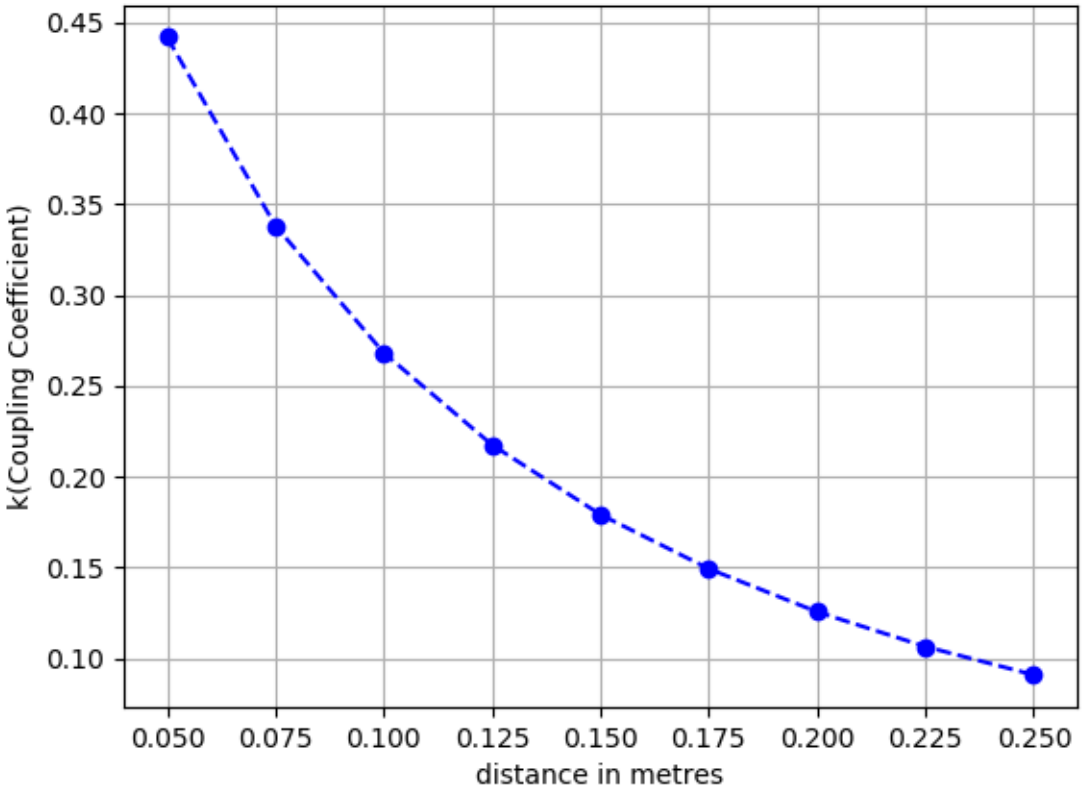

Figure 2.9: Coupling coefficient Vs Distance

2.5.3 Coupling coefficient vs distance

Now that we have calculated both self inductance and mutual inductance, coupling coefficient can be obtained by plugging in the values in eq. 1.1. If we assume that both the coils have same physical attributes then $k = \frac{M_{coil}}{L_{coil}}$
fig. 2.9 is obtained using the values in table 2.2. The plot is obtained using python. From the plot, it is evident that k goes below 0.1 after 0.225m. Therefore for the values in table 2.2 the maximum operable distance is 22.5cm.

N	a	ρ	δ_{xy}
11	42.55cm	1.415	0.270mm

Table 2.2: Parameters used for calculation of k

2.5.4 Code written for calculation of k

```
"""
Length of square coil = a = 42.55cm
Radius of each wire = r = 1.415 mm
Gap betweentwo wires = d = 0.27mm
Distance between centres of two wires = D
Number of turns in each coil = 11
Self inductance of coil = Lc
Mutual inductance between two coils = Mc

"""
import math
import numpy as np
import matplotlib.pyplot as plt

def L(l,r):
    c1 = math.sqrt(pow(l,2)+pow(r,2))
    return mu*2*((l*math.log((l+c1)/r))+r-c1+l/4)

def M(l,d):
    c2 = math.sqrt(pow(l,2)+pow(d,2))
    return mu*2*((l*math.log((l+c2)/d))+d-c2)



mu = pow(10,-7)
N = 11
r1 = 1.415e-3
d = 0.27e-3
D = 2*r1 + d
a = 42.55e-2


Lw = 0
```

```
for i in range(N):
    l = a-2*i*D
    Lw = Lw + L(l,r1)
A = a - (N-1)*D
Di = np.zeros((N,N))
Dij = np.zeros((N,N))
for i in range(N):
    for j in range(N):
        Di[i][j] = abs(i-j)*D
        Dij[i][j] = a - (i+j)*D
Mss = 0
Mos = 0
for i in range(N):
    for j in range(N):
        if j==i :
            Mos = Mos + M(A,Dij[i][j])
        else :
            Mss = Mss + M(A,Di[i][j])
            Mos = Mos + M(A,Dij[i][j])

Lc = 4*(Lw+Mss-Mos)

def Mc(A,h):
    Dik = np.zeros((N,N))
    Dit = np.zeros((N,N))
    for i in range(N):
        for k in range(N):
            Dik[i][k] = math.sqrt(pow(h,2)+pow((i-k)*D,2))
            Dit[i][k] = math.sqrt(pow(h,2)+pow(a-(i+k)*D,2))
    M1 = 0
    M2 = 0
    for i in range(N):
        for k in range(N):
```

```
            M1 = M1 + M(A,Dik[i][k])
            M2 = M2 + M(A,Dit[i][k])
    return 4*(M1-M2)


H = np.arange(50e-3,275e-3,25e-3)
Mi = [Mc(A,H[0]),Mc(A,H[1]),Mc(A,H[2]),Mc(A,H[3]),Mc(A,H[4]),Mc(A,H[5]
print("Mutual Inductance is", Mi[3]*pow(10,6))
print("Self Inductance of single coil is",Lc*pow(10,6))
print("Coupling coefficient is",Mi[3]/Lc)

plt.plot(H,Mi/Lc,'bo--')
plt.xlabel("distance in metres")
plt.ylabel("k(Coupling Coefficient)")
plt.grid()
plt.show()
```

2.6 Readout scheme based on FFT

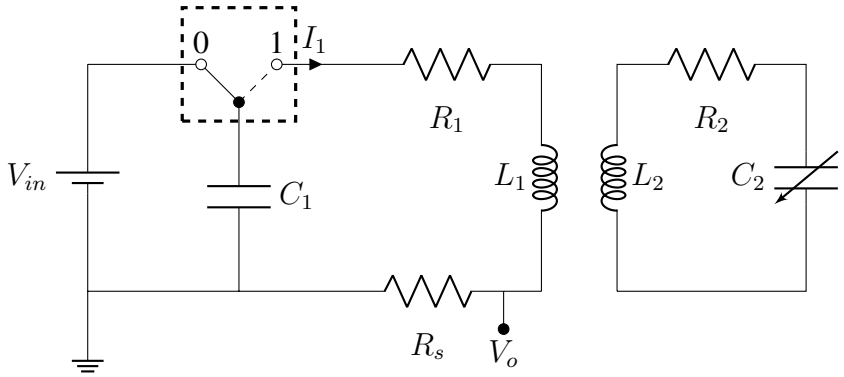

Figure 2.10: Circuit of the readout scheme based on FFT

This method is based on FFT of an input current based on impulse input and it exploits the fact that, for this system, imaginary part of input impedance, Z(s), is maximum at resonance frequency.

In fig. 2.10 capacitor C_1 is charged to predefined value. To measure value of C_2, C_1 is discharged through the readout coil which results in an oscillating and exponentially

decaying current through the coil. The frequency of oscillation depends on natural frequencies of the system, one of them is parallel resonance frequency. The voltage at V_o is proportional to the input current, I_1. The FFT of the V_o is taken and input impedance is computed from it.

$$V_o(s) = R_s I_1(s) = \frac{R_s V_{in}}{Z(s)} \tag{2.18}$$

An n-point FFT of V_o is computed. The FFT will have n complex terms and each complex term $V_k = \alpha_k + j\beta_k$. If we assume $R_s V_{in} = 1$, then[3]

$$Z_k = \frac{\alpha_k - j\beta_k}{\alpha_k^2 + \beta_k^2} \tag{2.19}$$

L_1	C_1	R_1	L_2	R_2
$13.3\mu H$	$1nF$	2.9Ω	$6\mu H$	9.9Ω

Table 2.3: Parameters used for calculation

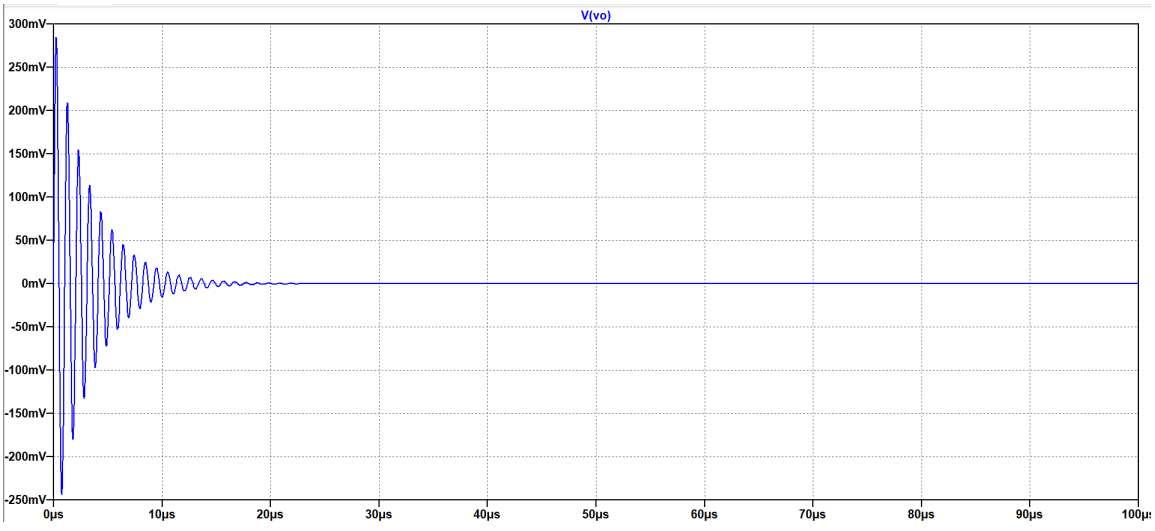

Figure 2.11: Output voltage obtained across the resistor R_s

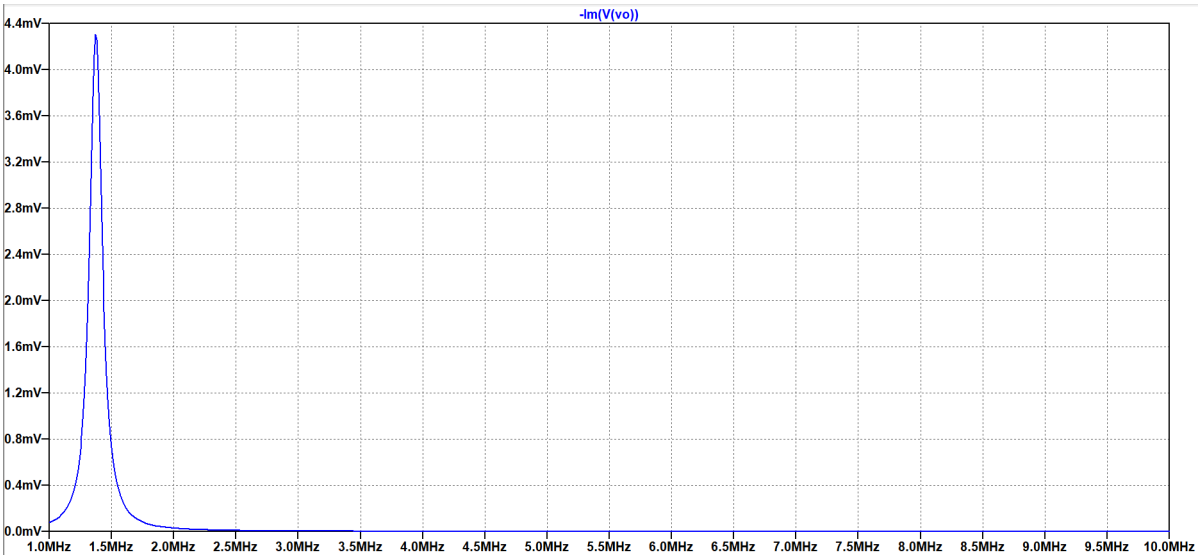

Figure 2.12: Maximum occurs at parallel resonance frequency

We can find f_p from this and as L_2 is already known. We can calculate the value of C_2.

This readout scheme does not require frequency sweep, so the measurement time is low. Therefore fast update rates can be achieved. The effect of k is also less. But it is affected by external noise. Real life V_o has some noise. Digitizing it also introduces quantization noise in the signal. To quantify these effects, we added white noise to V_o and simulated. Different peaks around f_p can be seen in fig. 2.13. We can overcome this problem by fitting a two term Gaussian curve to the plot. In this way all the unwanted peaks can be removed and we are left with a smooth curve as seen in fig. 2.13.

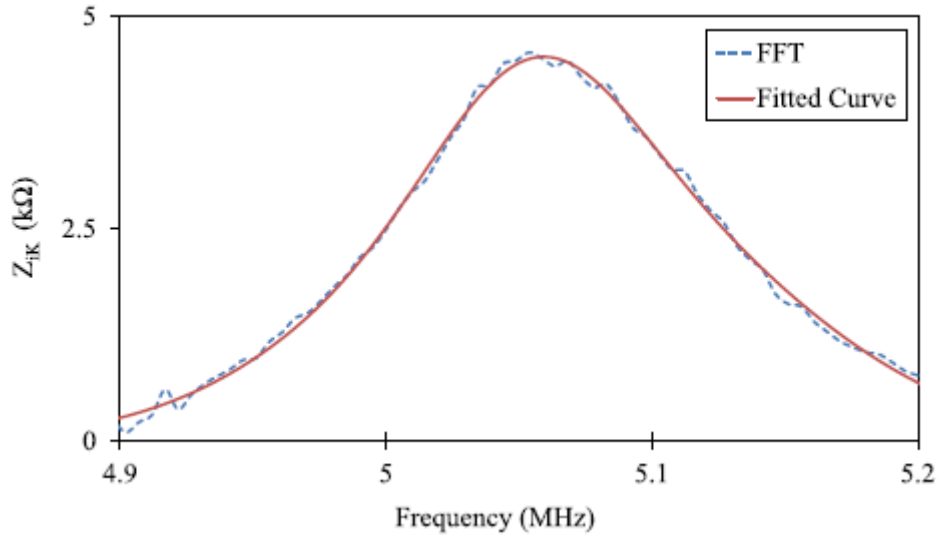

Figure 2.13: Peaks around f_p when noise is added and the Fitted curve in red[3]

CHAPTER 3

CONCLUSION

In this project, we have studied and analyzed various effects of interference on Passive LC sensors. We have also provided a code to calculate the mutual inductance between coils and plot the variation of coupling coefficient with distance.
Further this work can be continued on to the systems where we have both signal and power transfer. Our work on interference can be used, up to some extent, in studying such systems too. Because there shall be interference on sensing part as well as the readout circuit due to the transfer of different signals.

APPENDIX A

REFERENCES

1. Anish Babu and Boby George, Member, IEEE A Linear and High Sensitive Interfacing Scheme for Wireless Passive LC Sensors. *IEEE SENSORS JOURNAL*, Volume 16, No. 23, December 1 (2016).

2. Anish Babu and Boby George, Member, IEEE An FFT Based Readout Scheme for Passive LC Sensors. *IEEE Instrumentation and Measurement Society*,(2017).

3. Anish Babu and Boby George, Member, IEEE An Efficient Readout Scheme for Simultaneous Measurement From Multiple Wireless Passive LC Sensors. *IEEE SENSORS JOURNAL*, Volume 67, No. 5, May (2018).

4. Francisco Javier López-Alcolea , Member, IEEE, Javier Vázquez del Real, Pedro Roncero-Sánchez , Senior Member, IEEE, and Alfonso Parreño Torres Modeling of a Magnetic Coupler Based on Singleand Double-Layered Rectangular Planar Coils With In-Plane Misalignment for Wireless Power Transfer. IEEE TRANSACTIONS ON INSTRUMENTATION AND MEASUREMENT, *IEEE SENSORS JOURNAL*, Volume 35, No. 5, May (2020).